In situ pilot application of nZVI embedded in activated carbon for remediation of chlorinated ethene-contaminated groundwater: effect on microbial communities

Marie Czinnerova[1], Nhung H. A. Nguyen[1], Jan Nemecek[1], Katrin Mackenzie[2], Christopher Boothman[3], Jonathan Lloyd[3], Tamas Laszlo[4], Roman Spanek[1], Miroslav Cernik[1] and Alena Sevcu[1*]

Abstract

Background: Nanoscale zero-valent iron (nZVI) is commonly used for remediation of groundwater contaminated by chlorinated ethenes (CEs); however, its long-term reactivity and subsurface transport are limited. A novel nZVI–AC material, consisting of colloidal activated carbon (AC) with embedded nZVI clusters, was developed with the aim of overcoming the limitations of nZVI alone.

Results: Application of a limited amount of nZVI–AC to an oxic, nitrate-rich, highly permeable quaternary aquifer triggered time-limited transformation of CEs, with noticeable involvement of reductive dechlorination. Reductive dechlorination of CEs was dominantly abiotic, as an increase in the concentration of vinyl chloride (VC) and ethene did not coincide with an increase in the abundance of reductive biomarkers for complete dechlorination of CEs (*Dehalococcoides*, *Dehalogenimonas*, VC reductase genes *vcrA* and *bvcA*). Application of nZVI–AC under unfavourable hydrochemical conditions resulted in no dramatic change in the microbial community, the reducing effect resulting in temporal proliferation of nitrate and iron reducers only. At a later stage, generation of reduced iron induced an increase in iron-oxidizing bacteria. High concentrations and a continuous mass influx of competing electron acceptors (nitrate and dissolved oxygen) created unfavourable conditions for sulphate-reducers and organohalide-respiring bacteria, though it allowed the survival of aerobic microorganisms of the genera *Pseudomonas*, *Polaromonas* and *Rhodoferax*, known for their ability to assimilate VC or *cis*-1,2-dichloroethene. A potential for aerobic oxidative degradation of CE metabolites was also indicated by detection of the ethenotroph functional gene *etnE*.

Conclusions: This pilot study, based on the application of nZVI–AC, failed to provide a sustainable effect on CE contamination; however, it provided valuable insights into induced hydrogeochemical and microbial processes that could help in designing full-scale applications.

Keywords: nZVI–AC, nZVI, Chlorinated ethenes, Reductive dechlorination, Organohalide-respiring bacteria, Microbial community, Next generation sequencing

Background

Chlorinated ethenes (CEs), which include tetrachloroethene (PCE), trichloroethene (TCE) and their toxic metabolites, constitute a large environmental problem due to their persistence in the environment [1]. In recent years, nanoscale zero-valent iron (nZVI) has

*Correspondence: alena.sevcu@tul.cz
[1] Institute for Nanomaterials, Advanced Technologies and Innovation, Technical University of Liberec, Studentská 2, 461 17 Liberec, Czech Republic
Full list of author information is available at the end of the article

Czinnerova *et al. Environ Sci Eur* (2020) 32:154

Page 2 of 15

proved effective in CE treatment when employing two major reaction mechanisms, reductive dechlorination (hydrogenolysis) and reductive β-elimination. During reductive dechlorination, C–Cl bonds in CEs are sequentially replaced by C–H bonds to form Cl^- and less chlorinated CEs. During reductive β-elimination of CEs, triple bonds are created between carbon atoms and halogens are simultaneously removed from molecules in the form of Cl^- [2]. However, the high but short-term reactivity of bare nZVI particles, together with scanty subsurface transport due to their fast aggregation and agglomeration, limit the use of nZVI in remediation processes [3, 4]. Recently, the use of novel particles consisting of colloidal activated carbon (AC) with embedded nZVI structures (nZVI–AC) has significantly improved the properties of nZVI for in situ groundwater remediation [5], and these have successfully been used in early pilot-scale field tests [6, 7].

The negative surface charge of the nZVI–AC particles prevents the particles becoming immobilized in the near-neutral aquifer environment, which normally has a negative charge. Moreover, the AC acts as a spacer between individual nZVI particles, reducing the tendency of nZVI–AC particles to aggregate, leading to higher sedimentation stability of nZVI–AC suspensions, even at higher particle concentrations. In addition, suspension stabilizers used during injection, such as carboxymethyl cellulose (CMC), improve the mobility of particles in the subsurface layers. Due to a relatively weak sorption of CMC onto the nZVI–AC surface, CMC is steadily desorbed in the contact with fresh groundwater after injection [8]. The solubility of CMC in water is also important in this context, the recommended maximum molecular weight is < 10 kDa and a substitution degree between 0.6 and 1.0 [8]. Previous field studies in anoxic aquifers have shown particle transport distances of several metres and a high rate of PCE decomposition with no vinyl chloride (VC) formation [5, 6, 8].

Enhanced anaerobic biodegradation by organohalide-respiring bacteria (OHRB) is a process commonly used for the remediation of CEs at polluted sites. This method relies on reductive dechlorination, where CEs serve as electron acceptors and molecular hydrogen and acetate, both released as by-products of organic substrate fermentation reactions, are used by the dechlorinating bacteria as electron donors and carbon sources, respectively [9]. nZVI application has been shown to improve groundwater conditions, making them more favourable for OHRB by lowering the oxidation–reduction potential (ORP), depleting oxygen and nitrate from the groundwater and producing molecular hydrogen during its corrosion process, which serves as an electron donor

for chlorine removal during the organohalide respiration process [10, 11].

Although nZVI toxicity to microorganisms has been demonstrated in laboratory studies [12–14], field studies show only mild or short-term impacts on indigenous bacterial populations [15–17]. OHRB include a range of bacterial genera, including *Desulfitobacterium*, *Dehalobacter*, *Geobacter* and *Sulfurospirillum*, all of which utilize different reductases that can dechlorinate PCE to TCE and *cis*-1,2-dichloroethene (cDCE) [18]. However, only *Dehalococcoides* and *Dehalogenimonas* spp. are able to carry out the final and crucial step of CE degradation by dechlorinating cDCE via VC to non-toxic ethene [19, 20], using the specific VC reductases vcrA and bvcA [21].

In addition to anaerobic reductive dechlorination, degradation of CEs can also occur under aerobic conditions, either metabolically, where CEs are used as electron donors for cell growth, or by co-metabolism, where CEs are degraded fortuitously during the metabolism of other growth substrates, without gaining carbon or energy for bacterial growth [18]. Aerobic cometabolic degradation has been shown for all CEs, though only rarely described for PCE [22], and is related to certain aerobic bacteria, such as ethene oxidizers (ethenotrophs) and methane oxidizers (methanotrophs) [23–25]. Pure ethenotrophic strains of the genera *Mycobacterium* and *Nocardioides* can also degrade VC metabolically as their sole carbon and energy source [24], while *Polaromonas* sp. strain JS666 is the only microorganism known so far that is capable of oxidizing cDCE metabolically [26, 27]. A successful remediation treatment of a CE-polluted site in Lower Saxony (Germany) [7] showed how nZVI–AC injection could create conditions suitable for OHRB, with PCE subsequently dechlorinated to cDCE, though the subsequent cDCE degradation step was accomplished by an aerobic *Polaromonas* strain.

The purpose of this study was to examine the potential of novel nZVI–AC for cleaning a CE-polluted site and to elucidate abiotic and biotic processes triggered by nZVI–AC application and their impact on indigenous microorganisms.

Material and methods
Description of the study site
The pilot site, in the urban core of Balassagyarmat in Hungary, produced industrial electrical components between 1970 and 1994, but is mostly an industrial brownfield now. Geologically, the site comprises Quaternary alluvial sediments underlain by a sandstone bedrock weathered to silty fine-grained sand in its upper section. A two-layered aquifer system has developed in the Quaternary sediments, the upper layer consisting of Holocene fine-grained sand with a saturated thickness of

Czinnerova *et al. Environ Sci Eur*   (2020) 32:154

Page 3 of 15

7 m and the lower layer consisting of Pleistocene coarse-grained sand and sandy gravel with a total thickness of 3 m (Fig. 1). The upper and lower layers are separated by a semipermeable layer of silt and silty sand 3 m thick. The upper layer is overlain by sandy-clay to clayey-sand of low permeability, approximately 2 m thick. The upper and lower layers have a hydraulic conductivity of $5.0 * 10^{-6}$ m/s and $5.0 * 10^{-3}$ m/s, respectively, based on pumping tests. Estimated groundwater flow velocities are approximately 0.01 m/day in the upper layer and 10 m/day in the lower layer.

The polluted groundwater plume, which is approximately 250 m wide (East–West) and 700 m long (North–South), is primarily contaminated with PCE, TCE and metabolites of reductive dechlorination—cDCE and VC present as minor co-contaminants. The volume of contaminated groundwater is estimated at about 190,000 m^3, and the plume is believed to contain around 15 kg of CEs (95 wt% PCE). Highest contaminant concentrations of between 85 and 120 μmol/L CEs (14–20 ppm PCE) were found in the coarse sandy–gravelly lower layer at 12 to 13 m below ground level (bgl). The groundwater of both layers was oxic (concentration of dissolved O_2 ranging from 5.2 to 6.2 mg/L) of the Ca-HCO_3^- type, with elevated mineralisation (total dissolved solids ranged from 900 to 1185 mg/L) and slightly alkaline (pH 7.3–7.4).

Continuous multichannel wells (CMT wells) were installed on site (Fig. 2), each with two tubes, separated by bentonite packers to ensure representative sampling, the depth and screening interval being different for each

tube. The down-gradient CMT wells were monitored to examine the impact of nZVI–AC injection on groundwater conditions. Only in the closest down-gradient wells CMT 1 and CMT 2 the impact of nZVI–AC application was noticeable, therefore the suit of laboratory analyses of samples from these wells were extended with molecular biological tests and the whole dataset was assessed. Well CMT 1 was screened to a depth interval of 8.6–9.6 m bgl, representing the layer of fine-grained sand, whereas the well CMT 2 was screened at 13.4–14.4 m bgl, representing the lower course-grained sand and gravel layer. The up-gradient well, termed 14/04 (Fig. 2), was used to monitor the inflowing groundwater at a depth interval of 10.9–15.6 m bgl) and acted as a control.

nZVI–AC particles and injection parameters

nZVI–AC is an air-stable powder developed at the Helmholtz Centre for Environmental Research (UFZ; Germany), and is produced on an industrial scale by ScIDre GmbH (Germany). nZVI–AC consists of activated carbon colloids ($d_{50} \approx 1$ μm) with embedded nZVI structures with a mean Fe^0 content of 25 wt% [8]. Soluble CMC 75a was obtained from TiKEM (Hungary).

The nZVI–AC/CMC suspension used in this study was prepared by dispersion of the solid material in oxygen-free tap water under nitrogen atmosphere directly at the site. The suspension was injected by a Hydra-Cell G-10 hydraulic membrane pump (Wanner, UK) to a depth of 13 m bgl at three different injection points (Fig. 2) using TG63-150 penetrometer (Pagani,
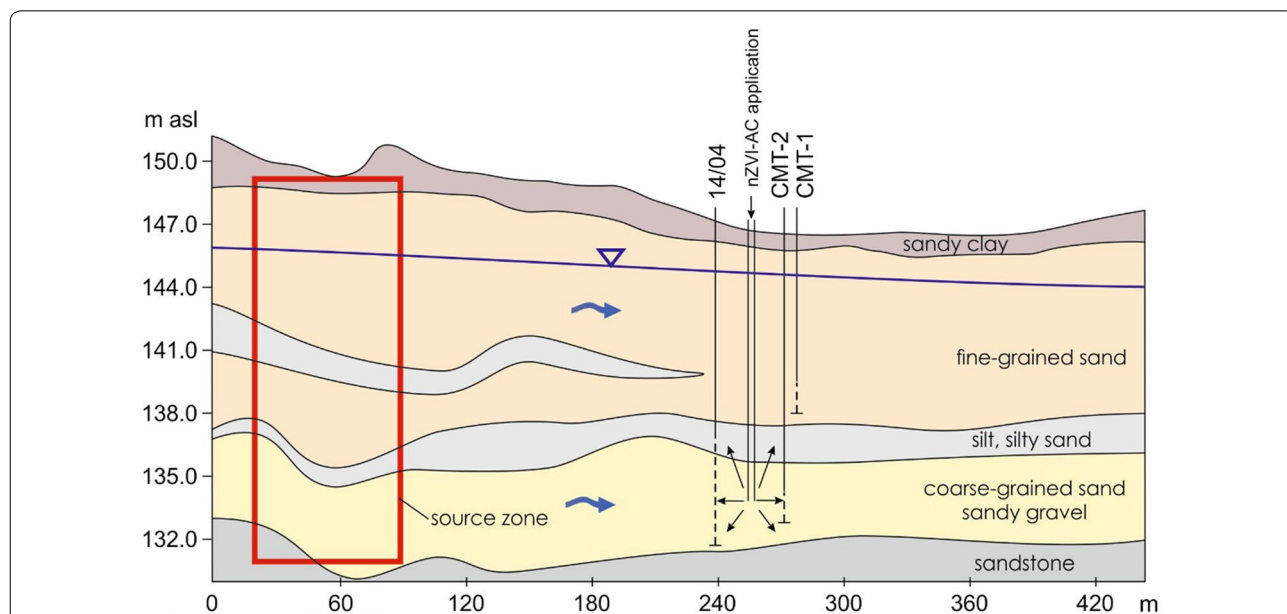

Fig. 1 Schematic geological cross section showing CEs source zone (red rectangle), up-gradient well 14/04, nZVI–AC application and down-gradient wells CMT 1 and CMT 2
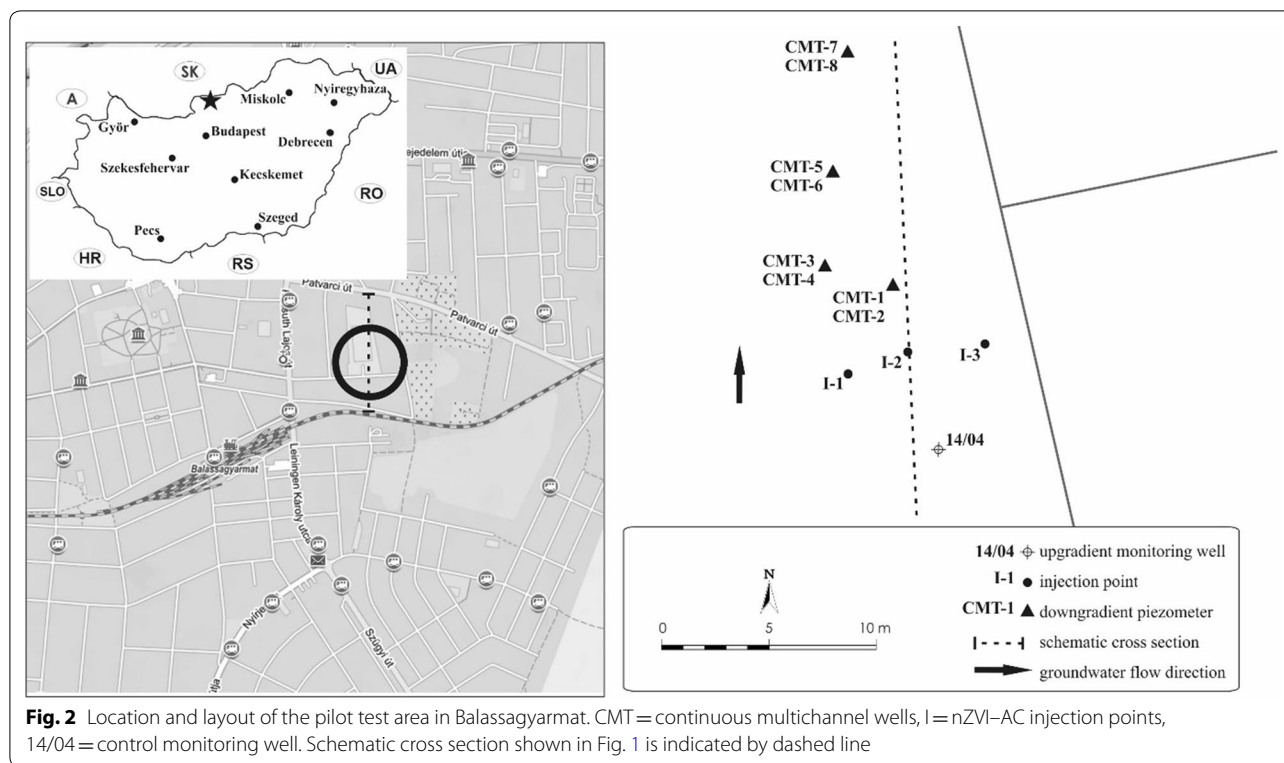
Czinnerova *et al. Environ Sci Eur*   (2020) 32:154

Page 4 of 15

Fig. 2 Location and layout of the pilot test area in Balassagyarmat. CMT = continuous multichannel wells, I = nZVI–AC injection points, 14/04 = control monitoring well. Schematic cross section shown in Fig. 1 is indicated by dashed line

Table 1 Parameters of in situ nZVI–AC injection

Parameter	Dimension
nZVI–AC	176.8 kg
Fe^0 (25% in nZVI–AC)	44.2 kg
CMC	21.2 kg
Oxygen-free tap water	12.35 m^3
nZVI–AC concentration	~14.3 g/L
CMC concentration	~1.7 g/L
Injection pressure	0.5–4 bar
Injection flow rate	20–30 L/min
Injection depth at each injection point	13 m bgl
Soil porosity	30%

Italy) and Geoprobe pressure activated injection probe rods (Geoprobe Systems®, USA). The composition of nZVI–AC/CMC suspension and specific injection parameters are summarized in Table 1.

nZVI–AC injection took place in September 2015, with one groundwater sampling campaign undertaken prior to nZVI–AC application and three sampling campaigns taking place over an 85-day period after injection.

Measurement of chemical and physical parameters

Water samples were obtained using a low-flow technology Gigant pump (Eijkelkamp, Netherlands). Physico-chemical parameters were analysed directly in the field with groundwater level measured using a Heron interface meter (Heron Instruments, Canada), pH, dissolved oxygen, oxidation–reduction potential (ORP; recalculated to the standard hydrogen electrode (ORP_H)) and electrical conductivity measured with a Multi 350i multimeter (WTW, Germany). Concentration of nitrate and sulphate ions was analysed according to EPA method 9056A:2007 and concentration of total dissolved iron according to EPA method 6010C:2007. Concentration of PCE, TCE, cDCE and VC was assessed using an HP-7890 gas chromatography–mass spectrometer (GCMS; Agilent Technologies, Inc., USA) and concentration of ethene and ethane with an HP-5890 gas chromatograph with a flame-ionisation detector and thermal conductivity detectors (Agilent Technologies, Inc., USA). Reductive dechlorination of parent PCE by less chlorinated products to non-CE was expressed by the chlorine number (Cl no.), which was calculated as the weighted average number of Cl atoms per molecule of ethene [28].

Czinnerova *et al. Environ Sci Eur*   (2020) 32:154

Page 5 of 15

DNA extraction and qPCR

Water samples for molecular genetic analysis were processed for DNA extraction immediately after sampling. The samples (0.5 l) were filtered through a 0.22 μm membrane (Merck Millipore, Germany) then DNA was extracted from the filter using the FastDNA Spin Kit for soil (MP Biomedicals, USA), according to the manufacturer's protocol.

The relative abundance of the 16S rRNA gene (representing total bacterial biomass), *Dehalobacter* spp., *Dehalococcoides* spp.*, Dehalogenimonas* spp., *Geobacter* spp., *Desulfitobacterium* spp., *Gallionella*, *Geobacter*, the VC reductase genes *vcrA* and *bvcA* and functional genes encoding enzymes for ethenotroph-mediated aerobic biodegradation [i.e. alkene monooxygenase (*etnC*) and epoxyalkane:coenzyme M transferase (*etnE*)] were determined by qPCR, as described previously [29]. Briefly, qPCR reactions were prepared and performed in a LightCycler® 480 instrument (Roche, Switzerland). Crossing point (Cp) values were obtained using the Second Derivative Maximum method. The qPCR results were evaluated as relative quantification of the fold change between two states, with the condition of specific bacteria or genes prior to application taken as the starting point. Average Cp values (normalised to sample volume) of a given marker were summarised following calculation described in Nechanicka et al. [30]. The Cp values were first divided into two sets, one with values lower than 36 and the other with values equal to or higher than 36. The first set of values was divided into three intervals of the same size, with lowest values classified as 'high quantity', mean values classified as 'intermediate quantity'; values equal to or higher than 36 classified as 'low quantity', values between 36 and 39 classified as 'detection limit' and values equal to 40 classified as 'not detected'. All primers used for qPCR are listed in Additional file 1: Table S1.

16S rRNA sequencing

DNA for 16S rRNA sequencing (next generation sequencing, NGS) was extracted from a 30 mL sample using the MO BIO PowerWater DNA Isolation Kit (Carlsbad, California, USA). The 16S rDNA gene was amplified via PCR using the 8F (5′-AGAGTTTGATCC TGGCTCAG-3′) and 1492R (5′-TACGGYTACCTTGTT ACGACTT-3′) primers [31]. Following PCR amplification, the DNA was stained and then placed in agarose gel, where it was subsequently separated using electrophoresis. The stained DNA was viewed under UV light and target ~ 1500 base pair products identified by comparison to a ladder of DNA fragments of varying lengths. Sequencing of the PCR amplicons for 16S rRNA was conducted using the Illumina MiSeq platform (Illumina, San Diego, CA, USA) by targeting the V4 hyper-variable region (forward primer, 515F, 5′-GTGYCAGCMGCCGCGGTAA-3′; reverse primer, 806R, 5′-GGACTACHVGGGTWT CTAAT-3′) for 2×250-bp paired-end sequencing (Illumina) [31, 32]. PCR amplification was performed using the Roche FastStart High Fidelity PCR System (Roche Diagnostics Ltd, Burgess Hill, UK) on 50-μL reactions under the following conditions: initial denaturation at 95 °C for 2 min, followed by 36 cycles of 95 °C for 30 s, 55 °C for 30 s, 72 °C for 1 min and a final extension step of 5 min at 72 °C. The PCR products were purified and normalised to ~ 20 ng each using the SequalPrep Normalization Kit (Fisher Scientific, Loughborough, UK). The PCR amplicons for all samples were then pooled in equimolar ratios. The run was performed using a 4 pM sample library spiked with 4 pM PhiX to a final concentration of 10%, following the method of Schloss and Kozich [33].

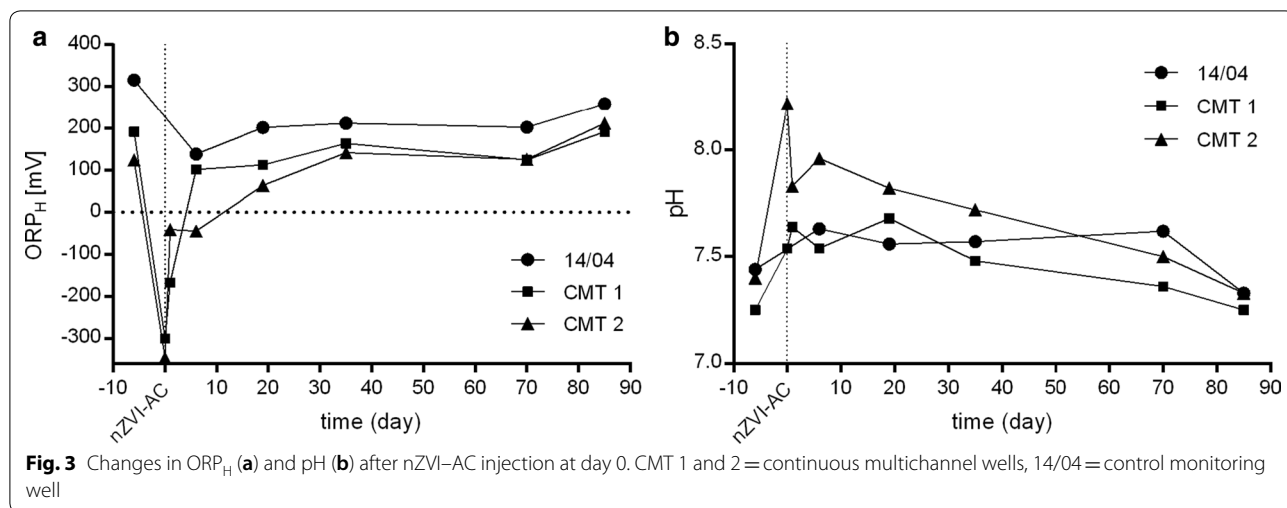## Sequencing data processing and analysis

Demultiplexed raw sequences were processed by DADA2 [34] following a standard DADA2 pipeline comprising (i) removal of low-quality and short reads, (ii) a search for and subsequent removal of chimeras (bimeras) and (iii) classification of reads against the SILVA reference database (version 13). Vegan [35] and phyloseq [36] R libraries were used for creation of the heatmap (only genera with a minimum relative abundance over 1% shown) and alpha-diversity comparison.

Results and discussion

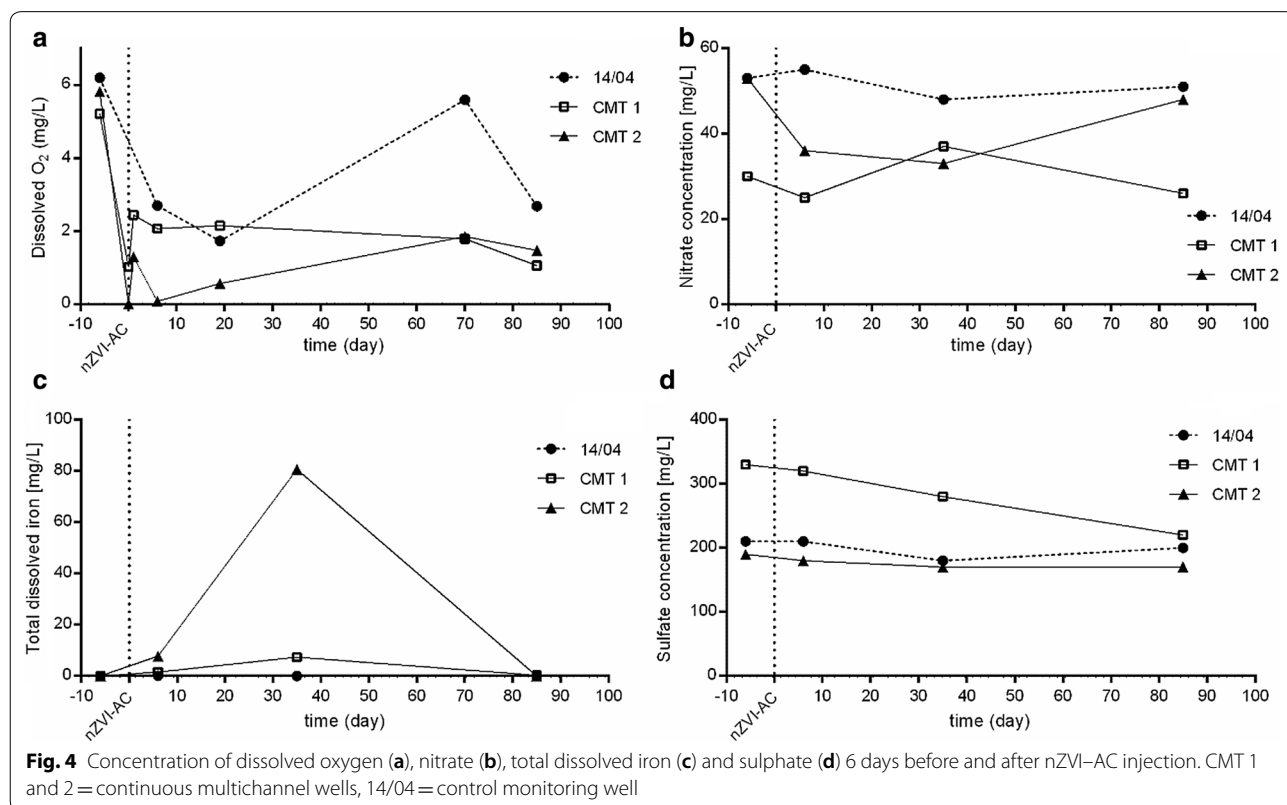### Groundwater physical and chemical parameters

Injection of nZVI–AC resulted in a rapid decrease in groundwater ORP from both layers in the CMT well (Fig. 3a). ORP_H dropped from 192 to $- 301$ mV in the upper layer (CMT 1) and from 125 to $- 347$ mV in the lower layer (CMT 2). Six days after injection ORP_H increased to 102 mV at CMT 1 and up to $- 45$ mV at CMT 2, screened to the layer where nZVI–AC was injected and, therefore, more affected. The nZVI–AC suspension tended to sink slightly during and shortly after injection (13 m bgl, with the injection bulb having an estimated radius of 1.5 m in sediment porosity); hence, CMT 1 (8.6–9.6 m bgl) in the upper aquifer horizon was naturally less affected by the particles over time. ORP_H in both layers then increased further, returning to levels similar to pre-injection on day 35. A slight but temporary decrease in ORP_H was also observed in the upgradient well 14/04.

Groundwater pH increased immediately after injection from an initial value of around 7.3 to 7.6 in in well CMT 1 to 8.2 in well CMT 2 due to a reaction between nZVI and dissolved oxygen and water that generated

Czinnerova *et al. Environ Sci Eur*   (2020) 32:154

Page 6 of 15

Fig. 3 Changes in ORP_H (**a**) and pH (**b**) after nZVI–AC injection at day 0. CMT 1 and 2 = continuous multichannel wells, 14/04 = control monitoring well

OH^- [2]. The pH of both layers had dropped to the initial level of approximately 7.3 at the end of the study on day 85 (Fig. 3b). A similar pH trend to that in CMT 1 was also observed in groundwater from the upgradient well 14/04, indicating a temporal effect of nZVI–AC injection on groundwater in nearby upgradient areas (discussed further below).

An initially high dissolved oxygen concentrations of 5.2 to 6.2 mg/L indicated oxic conditions in both the upper and lower aquifer layers (Fig. 4a). While such conditions lead to a shorter lifetime for the reactive function of the material, and hence are outside the recommended application window for abiotic CE treatment with nZVI–AC, we decided to proceed with the injection. After nZVI–AC application, depleted dissolved oxygen was only

Fig. 4 Concentration of dissolved oxygen (**a**), nitrate (**b**), total dissolved iron (**c**) and sulphate (**d**) 6 days before and after nZVI–AC injection. CMT 1 and 2 = continuous multichannel wells, 14/04 = control monitoring well

observed in the lower layer of CMT 2 on day 0; however, on the following day dissolved oxygen increased to 1.3 mg/L, and similar levels were observed for the rest of the pilot study. This was due to the inflow of oxic groundwater being higher than the reducing capacity of the nZVI–AC. In comparison, the effect of nZVI–AC on groundwater dissolved oxygen concentration in the upper layer of CMT 1 and in the upgradient area (14/04) was much lower (Fig. 4a).

The dynamics of nitrate concentration in both layers (Fig. 4b) suggested an insignificant, or at most temporary, effect of nZVI–AC on overall redox conditions. Nitrate concentration showed a dramatic decrease of 32% in lower layer groundwater up to day 35; however, levels had been re-established by the end of the study due to the high inflow of nitrate-rich groundwater and the weakening effect of nZVI–AC. The original concentration of dissolved iron (Fe) was close to its detection limit (0.1 mg/L) at this site (Fig. 4c). Application of nZVI–AC led to a significant increase in the upper and lower layers (7.4 and 80.7 mg/L, respectively) on day 35. This 35-day increase in soluble Fe(II) probably occurred as a consequence of a complexing effect between CMC and microbial processes, where CMC fermentation products or H_2 (produced by reaction of nZVI) acted as an electron donor with Fe(III) as the electron acceptor. These data are in accordance with our previous studies [16, 37], where we suggested that Fe(II) is derived not only from naturally present iron, but is also recycled from the injected nZVI that was oxidized to Fe(III). The effect of nZVI–AC on sulphate concentration in lower layer groundwater (Fig. 4d) was even lower than that observed for nitrate (Fig. 4b) as conditions suitable for microbial sulphate reduction were not established. The linear decrease of sulphate concentration detected in the upper layer of CMT 1 does not appear to be related to abiotic reduction by nZVI–AC.

As the presence of electron acceptors in groundwater, mainly dissolved oxygen and nitrate has the negative effect on the CE degradation by nZVI–AC, consumption of the reducing power of nZVI by the reduction of dissolved oxygen and nitrate was estimated as follows.

Consumption of electrons by a reduction of oxygen and nitrate was calculated using the appropriate reduction reactions [38]:
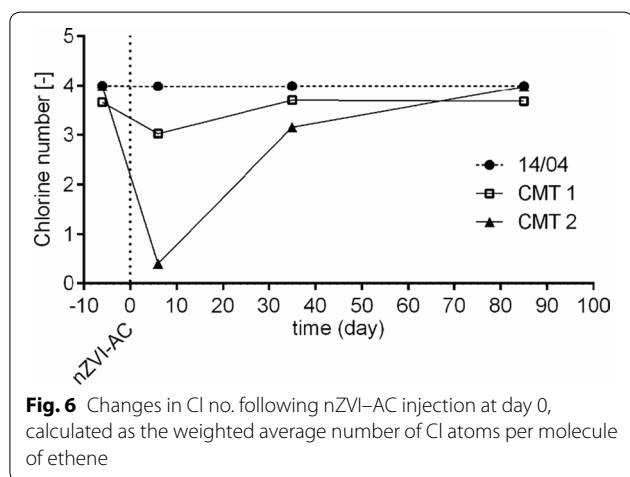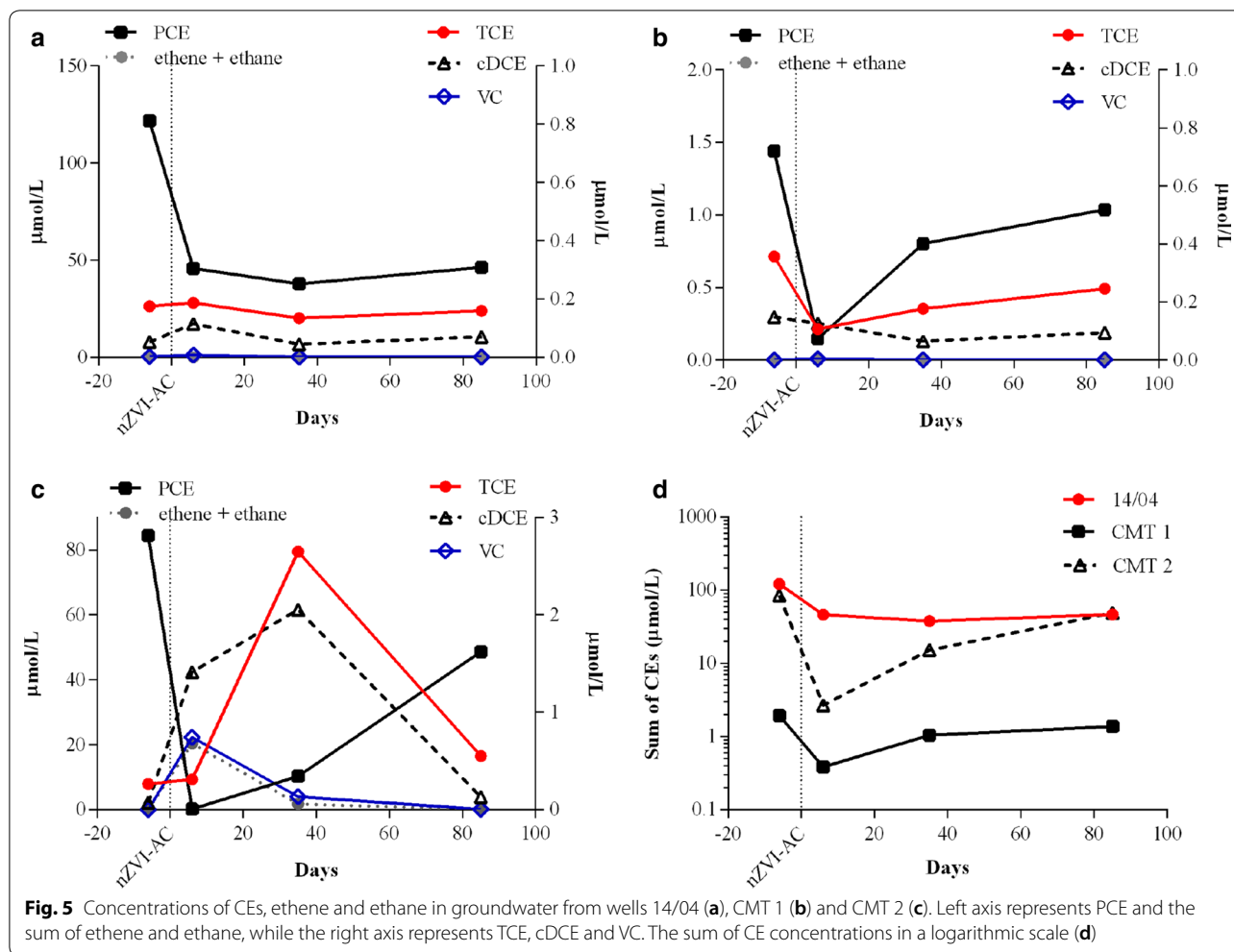
$$\frac{1}{2}O_2 + 2H^+ + 2e^- = H_2O$$

$$NO_3^- + 6H^+ + 6e^- = \frac{1}{2}N_2 + 3H_2O$$
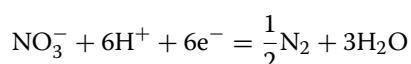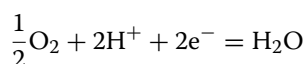
and a conservative assumption that the whole amount of applied nZVI–AC distributed in the lower layer with

radius of influence of 1.5 m filled the void space of effective porosity of 20% in the area of approximately 26 m^2 (3 m diameter × 8.7 m depth). By taking the groundwater flow velocity of 10 m/day, the reducing power of nZVI (total number of electrons potentially donated from Fe^0 oxidation to Fe^{3+}) was theoretically exhausted in 9 days on the chemical reduction of dissolved oxygen and nitrate flowing into the treatment zone. Even though CMC also provided the reducing power in the process of its biological degradation and the fact that not all amount of nitrate was reduced, it was evident that the amount of nZVI–AC was not sufficient for substantial and long-term degradation of CE.

Monitoring of PCE and its degradation products

While CE concentrations in groundwater from the upgradient control well (14/04) remained more-or-less stable throughout the study (Fig. 5a), those in groundwater from the upper layer of CMT 1 and the lower layer of CMT 2 were lower (Fig. 5b, c), having been affected by nZVI–AC application.

Highest initial PCE concentrations were detected in groundwater from upgradient well 14/04 (121.8 μmol/L) and in groundwater from the lower layer of CMT 2 (84.4 μmol/L), with just 1.4 μmol/L detected in the upper layer of CMT 1. A rapid decrease in PCE concentration was observed in both downstream layers (90% decrease in CMT 1 and 99.8% in CMT 2) 6 days after nZVI–AC injection, followed by a slow increase to 72% (CMT 1) and 58% (CMT 2) of the initial concentrations by the end of the field experiment (day 85) due to continuous inflow of contaminated groundwater. The Cl no. ranged from 3.7 to 4 prior to injection, reflecting a very low dechlorination level of the parent contaminant PCE (Fig. 6). In comparison, the Cl no. remained high (4.0) throughout the study in groundwater from control well 14/04, indicating that reductive dechlorination did not play a significant role in the groundwater around this well. Cl no. dynamics in CMT 1 and CMT 2 indicated that reductive dechlorination contributed noticeably to a temporal decrease in PCE concentration and the subsequent formation of daughter products. This process could either have been abiotic or, after a lag phase, biotic, the process being mediated by OHRB where H_2, originating from the reaction between nZVI and water, serves as an electron donor. In CMT 1, the Cl no. decreased slightly from 3.7 to 3.0, 6 days after nZVI–AC injection, but had returned to its initial level (Cl no. 3.7) by day 35. Reductive dechlorination in CMT 1 appeared rather weak, most likely due to limited migration of nZVI–AC into the upper layer, as also observed by Mackenzie et al. [6] at a different site. The lower layer (CMT 2) exhibited the greatest decline in Cl no., falling from a baseline of 4.0 to 0.4 after 6 days.

Czinnerova *et al. Environ Sci Eur* (2020) 32:154

Page 8 of 15

Fig. 5 Concentrations of CEs, ethene and ethane in groundwater from wells 14/04 (**a**), CMT 1 (**b**) and CMT 2 (**c**). Left axis represents PCE and the sum of ethene and ethane, while the right axis represents TCE, cDCE and VC. The sum of CE concentrations in a logarithmic scale (**d**)

Fig. 6 Changes in Cl no. following nZVI–AC injection at day 0, calculated as the weighted average number of Cl atoms per molecule of ethene

An increase in pH from a baseline of 7.4 to 8.2 on day 0 documented corrosion of nZVI by water. The gradual restoration of both Cl no. and CE concentration (Figs. 5d,

6) to their initial values by the end of the test indicates that the effect of nZVI–AC injection was temporary. This was probably due to the material itself having a limited lifetime, due mainly to a strong inflow of other electron acceptors (such as dissolved oxygen and nitrate) into the treatment zone, together with PCE from upgradient areas.

Initial levels of less chlorinated metabolites (TCE, cDCE and VC) were low throughout the aquifer. Maximal initial concentrations were 0.357 µmol/L for TCE, 0.149 µmol/L for cDCE in well CMT 1 and 0.003 µmol/L for VC in well CMT 2. Less chlorinated metabolite concentrations differed between wells. On day 6, TCE and cDCE concentrations decreased temporarily in well CMT 1, while VC concentration increased slightly then dropped below the detection limit until the end of the study, both confirming low level of reductive dechlorination in CMT 1.

Responses differed in the lower layer at well CMT 2, where TCE, cDCE and VC concentrations increased

alongside nZVI–AC injection and PCE degradation (Fig. 5c). On day 35, TCE had increased by a factor of 10 (3.2% of initial PCE concentration transformed) and cDCE by a factor of 28 (2.5% of the initial PCE), while VC had increased by a factor of more than 900 by day 6 (0.8% of PCE before injection). Subsequently, there was a decline in metabolite concentrations, though by the end of the study levels were still higher than initial readings.

In the upgradient well 14/04, concentrations of the less chlorinated metabolites TCE, cDCE and VC showed only minor changes, all within typical deviation limits for field studies (Fig. 5a). By day 6, the cDCE concentration had increased by a factor of 2.2 and VC concentration by a factor 2.5, though levels subsequently dropped to (cDCE) or below (VC) their initial levels.

The initial levels of both ethene and ethane (non-chlorinated metabolites of CE anaerobic degradation) were below detection limits (< 0.001 μmol/L) in both monitoring wells and, aside from CMT 2, did not change significantly over course of the study. In CMT 2, application of nZVI–AC resulted in a significant increase in ethene and ethane to 10.4 μmol/L and 10.0 μmol/L, respectively, by day 6, followed by a rapid decrease toward the end of the study (Fig. 5c).

Overall, nZVI–AC injection resulted in mild and short-term reductive dechlorination of CEs in the upper layer (CMT 1), and noticeable, though time-limited, changes in the lower layer (CMT 2). Previous studies have shown that, while biological reductive dechlorination of CEs can occur under both nitrate-reducing and iron-reducing conditions, sulphate reducing and methanogenic conditions are most favourable for OHRB [39]. Unfortunately, such conditions were not established at our site.

Bacterial community
Bacterial community prior to nZVI–AC application
The microbial community in the aquifer was characterized by a high abundance of genera known for their involvement in nitrogen geochemical cycles, including nitrite-oxidizing *Nitrospira*, ammonia-oxidizing Candidatus *Nitrosoarchaeum*, nitrate-reducing *Rhodoferax* and *Methylotenera,* and iron: iron-oxidizing *Gallionella* and *Sediminibacterium*, iron-reducing *Rhodoferax, Ferribacterium* and *Geobacter.*

In contrast, the abundance of sulphate-reducing bacteria detected by NGS in our dataset was very low. The families Desulfobulbaceae and Desulfovibrionaceae were only detected in well CMT 1, with no assigned genera (data not shown). On the other hand, the sulphur-oxidizing genus *Sulfuritalea* was found in all samples and was recorded at highest abundance in the lower zone of well CMT 2. Finally, qPCR revealed a higher initial abundance of *Desulfitobacterium* in well 14/04.

Noticeable differences in the initial abundance of OHRB and VC reductase genes were detected by qPCR in the upper and lower layers of groundwater. In general, a higher abundance of OHRB (comprising the genera *Dehalobacter*, *Dehalococcoides* and *Dehalogenimonas*) were found in the upper groundwater layer in CMT 1 than the lower layer in CMT 2. Low numbers of OHRB in the lower layer most likely relate to its high permeability and the high mass fluxes of oxygen and nitrate that inhibit organohalide respiration [40]. The slightly higher degree of PCE reductive degradation observed in the upper groundwater layer (Cl no. 3.7 in the upper layer compared to 4.0 in the lower layer, Fig. 6) may reflect the stratification of OHRB.

NGS analysis did not reveal the presence of any OHRB other than the genus *Dehalogenimonas*, the only assigned member of the phylum Chloroflexi (below 1% of total genera detected), the genera *Desulfitobacterium*, *Dehalobacter* and *Dehalococcoides* not being detected. Nevertheless, qPCR confirmed the presence of these OHRB, together with VC reductase genes, in the aquifer. A similar discrepancy between NGS and qPCR data has been reported previously [41, 42], the previous authors explaining this by both a very low relative abundance of OHRB in the bacterial community and more efficient PCR amplification using the highly specific qPCR primers rather than the universal primers used for NGS.

On the other hand, NGS did reveal the presence of *Trichococcus* in the lower layer of CMT 2, a bacterial genus capable of dechlorinating PCE and TCE with the TceA enzyme [43]. Furthermore, the groundwater in both layers contained the genus *Aquabacterium*, capable of dechlorinating under anaerobic conditions [44]. Similarly, the proteobacterial group MND1, which was abundant in well 14/04, and *Hydrogenophaga*, detected in high numbers in both layers of the CMT wells, have both been recorded in relation to remediation of contaminated soils [44, 45]. In reference well 14/04, *Pseudorhodobacter* were the most abundant bacterial genus; however, while the genus has previously been detected on sites contaminated with CEs [41], there is no evidence of its association with CE degradation.

NGS also detected several genera known for their ability to degrade CEs aerobically, namely *Polaromonas* and *Pseudomonas*. Bacteria of the genus *Polaromonas* are commonly found in groundwater samples at CE-contaminated sites, even in deep wells where anoxic conditions predominate [7, 41, 43, 46]. Interestingly, *Polaromonas* sp. strain JS666 is the only microorganism known to oxidize cDCE by using it as a sole carbon and energy source [26]. The genus *Pseudomonas* comprises

Czinnerova *et al. Environ Sci Eur*   (2020) 32:154

Page 10 of 15

strains capable of aerobic cometabolic PCE and TCE degradation and VC-assimilation [18, 24, 47].

Effect of nZVI–AC application

Soon after nZVI–AC injection, the bacterial genera *Rhodoferax* and *Ferribacterium,* both involved in iron reduction (*Rhodoferax* also respires with other electron acceptors, including nitrate), and *Methylotenera,* also involved in nitrate reduction, proliferated in both layers of in the CMT wells (Fig. 7). This increase is most likely related to the establishment of more favourable redox conditions and the availability of electron donors following application of the nZVI–AC/CMC suspension. The facultative anaerobe *Rhodoferax* has been shown to assimilate VC as a primary growth substrate [48]; further, it could regenerate iron for additional CE reduction by reducing oxidized Fe(III) to Fe(II).

Both iron-oxidizing *Gallionella* and iron-reducing *Geobacter* have previously been shown to dechlorinate PCE or TCE [49, 50]. In our study, *Gallionella*, which was initially found at a relatively high abundance in the upper layer of CMT 1, proliferated 1 day after nZVI–AC injection. However, a much greater increase was observed in the lower layer of CMT 2, 35 days after the injection (Table 2; Fig. 8). This corresponded with elevated levels of total dissolved iron (Fe(II)). *Gallionella* is commonly found in the groundwater of CE-contaminated sites [47, 51] and has been described as capable of dechlorinating

TCE under sulphate-reducing conditions [49]. While iron-reducing *Geobacter* were already abundant in well 14/04 and in the upper layer of CMT 1, their abundance increased even further after nZVI–AC application (Table 2; Fig. 8).

On the other hand, relative abundance of the iron-oxidizing genus *Sediminibacterium* declined over the course of the study (Fig. 7). This may have been caused by an increasingly complex microbial community structure over time, leading to increased interspecific competition.

Application of nZVI–AC resulted in a decrease in the abundance of sulphur-oxidizing *Sulfuritalea* in the upper and lower layers of the CMT well by day 6, followed by partial recovery (Fig. 7). *Desulfitobacterium* was the only sulphate-reducing bacteria detected in the aquifer; thus, we can assume that groundwater conditions were insufficiently reduced by nZVI–AC to support sustained growth of sulphate-reducing bacteria. This is also supported by the changes in groundwater sulphate concentrations, with the most significant changes in CE concentration being observed on day 6 in the lower layer CMT 2 and an increase in the abundance of *Desulfitobacterium,* known to degrade PCE down to cDCE (Table 2; Fig. 8). However, other reductive biomarkers were also found in similar (*Dehalobacter*, *Dehalogenimonas,* VC reductase gene *bvcA*) or lower (*Dehalococcoides,* VC reductase gene *vcrA*) levels (Table 2; Fig. 8), suggesting that reductive dechlorination of CEs was dominantly
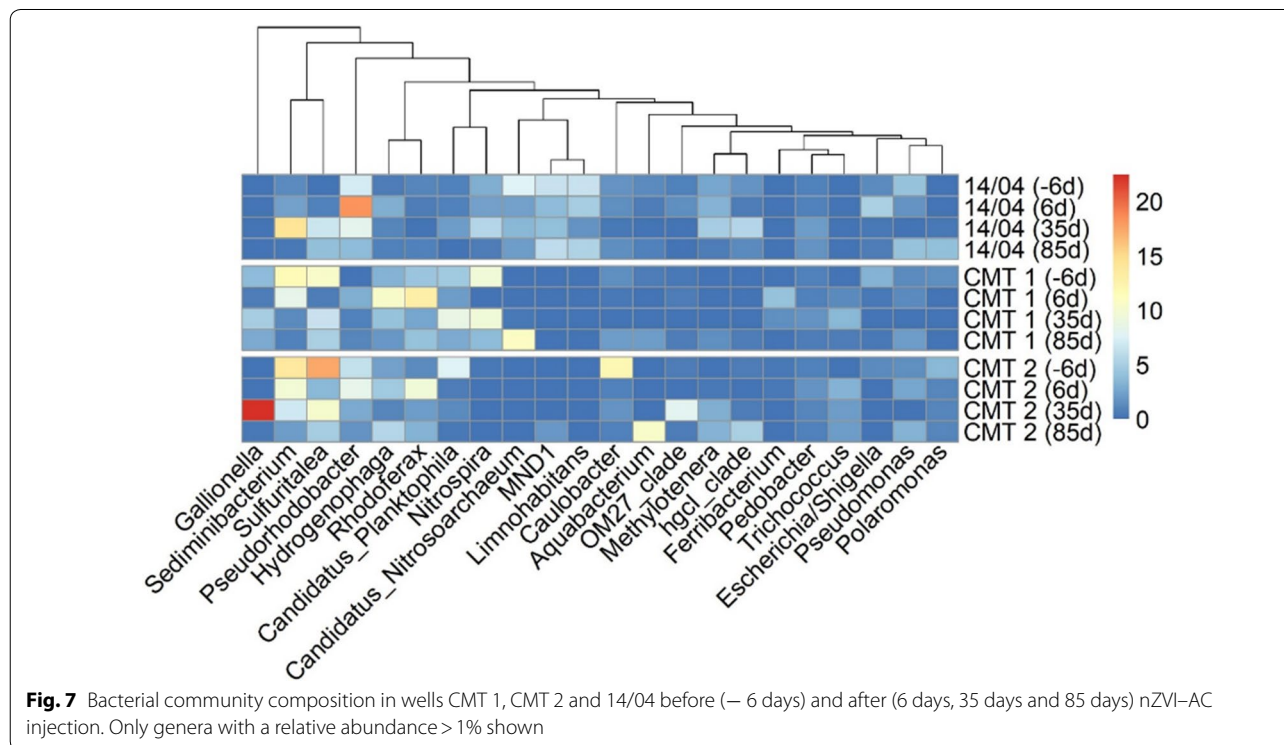

Fig. 7 Bacterial community composition in wells CMT 1, CMT 2 and 14/04 before (— 6 days) and after (6 days, 35 days and 85 days) nZVI–AC injection. Only genera with a relative abundance > 1% shown

Czinnerova *et al. Environ Sci Eur*   (2020) 32:154

Page 11 of 15

Table 2 Summary of qPCR results for changes in the relative abundance of biomarkers following nZVI–AC injection (day 0)

Well	Time before and after nZVI–AC injection (days)				
14/04	− 6	1	6	35	85
16S rRNA	++	+++	+++	++	+
Desulfitobacterium	+++	+++	+++	++	+
Dehalobacter	++	+++	+++	++	+−
Dehalococcoides	ND	ND	ND	ND	+
vcrA	ND	ND	ND	ND	+
bvcA	ND	ND	ND	ND	+++
Dehalogenimonas	++	+	+−	+−	+−
Gallionella	+	+	+	+	++
Geobacter	++	++	+++	+++	+
etnC	+++	++	+++	+++	+
etnE	+++	++	+++	++	+−
CMT 1					
16S rRNA	+	++	++	++	++
Desulfitobacterium	+	++	+++	+++	+++
Dehalobacter	++	+++	++	++	+++
Dehalococcoides	+++	+++	++	+++	+++
vcrA	ND	++	ND	+++	ND
bvcA	ND	+++	ND	ND	++
Dehalogenimonas	+++	+++	++	++	+++
Gallionella	++	+++	++	++	+++
Geobacter	+	+++	++	+	+++
etnC	+	+	+	+−	+
etnE	+	+−	+	+−	+−
CMT 2					
16S rRNA	+	+	+	++	+
Desulfitobacterium	+	+	+++	+	+++
Dehalobacter	+	++	+	+	++
Dehalococcoides	+	+	+−	+	+
vcrA	++	ND	ND	+	++
bvcA	ND	ND	ND	ND	ND
Dehalogenimonas	+	++	+	+	+
Gallionella	+	++	++	+++	++
Geobacter	+	+	+	+	+
etnC	+−	+−	+−	+−	+−
etnE	+	+++	+	+v	++

Calculations were based on Cp values, with +++ = high abundance; ++ = medium abundance; + = low abundance; +− = at detection limit; ND = not detected

abiotic and can be attributed to nZVI–AC application. The abundance of *Dehalobacter, Desulfitobacterium* and the gene *vcrA* showed an increasing trend up to day 85, though not enough to result in significant reductive dechlorination activity as the Cl no. also increased at the same time (Fig. 6).

OHRB and VC reductase genes were more abundant in the upper layer of CMT 1 (compared to the lower layer) throughout the study; however, their abundance increased even further following nZVI–AC injection. Nevertheless, OHRB activity in this layer did not exhibit significant and sustainable reductive CE dechlorination.
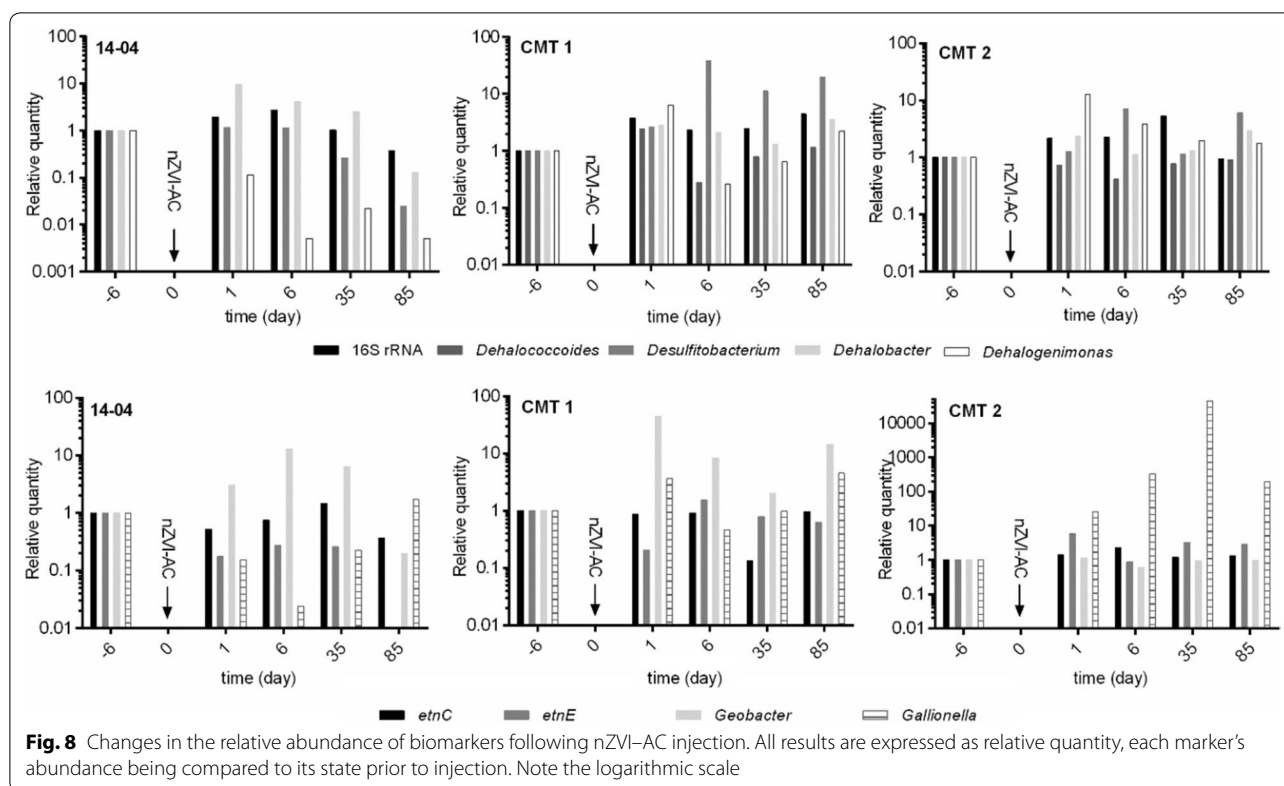
Of the bacteria potentially participating in CE dechlorination, *Trichococcus* increased in both aquifer layers, culminating on day 6 in the lower layer and day 35 in the upper layer, after which it decreased again but not to its initial levels. Bacteria of the genus *Aquabacterium* declined in both layers following nZVI–AC application. By the end of the study (day 85), however, they had proliferated remarkably (Fig. 7).

Of the bacteria potentially degrading CEs aerobically, *Polaromonas* abundance decreased in both aquifer levels following nZVI–AC application (Fig. 7); however, while it declined to non-detectable levels in the upper layer (CMT 1) it remained detectable in the lower layer (CMT 2) throughout the study, indicating a potential for oxidative degradation of CEs. Similarly, the genus *Pseudomonas* exhibited had decreased in abundance by day 35 in both aquifer layers, but had staged a distinct recovery by the end of the study (day 85; Fig. 7). A slight increase in the abundance of the ethenotroph functional gene *etnE* was detected on day 35, indicating the potential for aerobic oxidative degradation of VC and cDCE (Table 2; Fig. 8).

Overall, NGS failed to show dramatic changes in the microbial community induced by nZVI–AC application. Bacterial community alpha-diversity showed high between-sample similarity prior to nZVI–AC injection, with no significant differences found after injection (Additional file 1: Fig. S1). The reducing effect of nZVI–AC resulted in short-term proliferation of nitrate and iron reducers only, with the reduced iron generated inducing an increase in iron-oxidizing bacteria at a later stage.

Owing to high initial concentrations and continuous mass influx of nitrate and dissolved oxygen, conditions for sulphate-reducing microorganisms and OHRB were unfavourable. As reported previously [39], presence of electron acceptors other than CEs has an inhibitory effect on organohalide respiration. Nevertheless, while optimal redox conditions required for anaerobic OHRB (i.e. sulphate-reducing or methanogenic [37]) were not achieved, these bacteria were detected in all wells prior to, and at slightly increased numbers after, nZVI–AC injection.

On the other hand, low dissolved oxygen levels permitted the concurrent presence of OHRB and CE oxidizing *Pseudomonas* and *Polaromonas* (both capable of assimilating cDCE), which is in accordance with the first field-scale study by Vogel et al. [7], who observed

Czinnerova *et al. Environ Sci Eur*   (2020) 32:154

Page 12 of 15

Fig. 8 Changes in the relative abundance of biomarkers following nZVI–AC injection. All results are expressed as relative quantity, each marker's abundance being compared to its state prior to injection. Note the logarithmic scale

nZVI–AC-supported organohalide respiration of PCE complemented by the oxidative degradation of cDCE by *Polaromonas*, even in deep anoxic wells 25 m bgl. Furthermore, detection of the ethenotroph functional gene *etnE* indicated the potential for ethenotroph-mediated aerobic biodegradation of CE metabolites. Co-occurrence of OHRB and VC assimilating bacteria has also been found in groundwater [17, 52, 53] and discrete aquifer soil samples [25] at other sites.

Conclusions

This study describes the effect of application of an nZVI–AC composite on hydrochemical conditions and microbial community of an oxic aquifer. In doing so, we intended to elucidate the chemical and microbial processes involved in CE transformation.

The main findings are as follows:

Hydrochemical data indicated CE transformation with the noticeable involvement of reductive dechlorination.

Reductive dechlorination of CEs was primarily abiotic as an increase in ethene and low concentrations of VC did not coincide with an increase in the abundance of reductive biomarkers indicating complete dechlorination of PCE (*Dehalococcoides, Dehalogenimonas,* VC reductase genes *vcrA* and *bvcA*).

Hydrochemical parameters (a temporal decrease in groundwater dissolved oxygen concentration and an insignificant, or temporary, decrease in nitrate and sulphate concentration) indicated a limited, short-term effect of nZVI–AC application, probably due to a high overall inflow of competing electron acceptors (CEs and oxidized inorganic compounds) and the low levels of Fe(0) applied to the treatment zone. This is in accordance with the changes observed in the bacterial community, where reducing effects only resulted in temporary and/ or short-term proliferation of nitrate and iron reducers. The generated reduced iron induced an increase in iron-oxidizing bacteria at a later stage. Overall, we observed no significant inhibition effect of nZVI–AC on the bacterial community or its diversity.

Oxic conditions in the aquifer prevented any significant growth of strictly anaerobic OHRB such as *Dehalococcoides* and their functional VC reductase genes *vcrA* and *bvcA* in the treatment zone; however, it did allow the survival of aerobic microorganisms of the genera *Pseudomonas, Polaromonas* and *Rhodoferax*, known for their ability to assimilate VC or cDCE. A potential for aerobic oxidative degradation of CE metabolites was also indicated through the detection of the ethenotroph functional gene *etnE*.

Czinnerova *et al. Environ Sci Eur*   (2020) 32:154

Page 13 of 15

While this nZVI–AC application pilot study failed to produce a sustainable effect on CE contamination, it provided valuable insights into the hydrogeochemical and microbial processes induced, which could prove useful when designing full-scale applications.

Supplementary information

Supplementary information accompanies this paper at https://doi.org/10.1186/s12302-020-00434-2.

Additional file 1: Table S1. Specific primer pairs used for qPCR method. **Figure S1.** Alpha-diversity measures: comparison of wells based on Chao 1 and Inv. Simpson alpha-diversity indexes.

Abbreviations

AC: Colloidal activated carbon; bgl: Below ground level; cDCE: *cis*-1,2-Dichloroethene; CE: Chlorinated ethene; Cl no.: Chlorine number; CMC: Carboxymethyl cellulose; CMT: Continuous multichannel well; DNA: Deoxyribonucleic acid; NGS: Next generation sequencing; nZVI: Nanoscale zero-valent iron; OHRB: Organohalide-respiring bacteria; ORP: Oxidation–reduction potential; PCE: Tetrachloroethene; qPCR: Quantitative polymerase chain reaction; TCE: Trichloroethene; VC: Vinyl chloride.

Authors' contributions

LT, KM, JL, MC and AS designed the study. LT led in situ application of nZVI–AC and performed the chemical analysis. CB performed the 16S rRNA sequencing, NN and MC performed the qPCR analysis and RŠ analysed the data. MC, NN and JN wrote the draft manuscript, AS, KM and MC reviewed the manuscript. All authors read and approved the final manuscript.

Availability of data and materials

All data necessary to interpret and replicate the findings reported herein are included in the published article and its additional files. Other data used and/or analysed during the current study are available from the corresponding author on reasonable request.

Ethics approval and consent to participate

Not applicable.

Consent for publication

Not applicable.

Competing interests

The authors declare that they have no competing interests.

Author details

[1] Institute for Nanomaterials, Advanced Technologies and Innovation, Technical University of Liberec, Studentská 2, 461 17 Liberec, Czech Republic. [2] Department of Environmental Engineering, Helmholtz Centre for Environmental Research-UFZ, 04318 Leipzig, Germany. [3] School of Earth and Environmental Sciences, University of Manchester, Manchester M13 9PL, UK. [4] Golder Associates, Hüvösvölgyi út 54, 1021 Budapest, Hungary.

References

1. Tobiszewski M, Namieśnik J (2012) Abiotic degradation of chlorinated ethanes and ethenes in water. Environ Sci Pollut Res 19:1994–2006. https://doi.org/10.1007/s11356-012-0764-9
2. Černík M, Zeman J (2020) Geochemical principles of reductive remediation processes. In: Filip J, Cajthaml T, Najmanová P, Černík M, Zbořil R (eds) Advanced nano-bio technologies for water and soil treatment. Springer, Cham, pp 3–17
3. Phenrat T, Lowry GV (2019) Nanoscale zerovalent iron particles for environmental restoration: from fundamental science to field scale engineering applications. Springer, Berlin
4. Filip J (2019) Advanced nano-bio technologies for water and soil treatment. Springer, Berlin
5. Bleyl S, Kopinke F-D, Mackenzie K (2012) Carbo-Iron®—synthesis and stabilization of Fe(0)-doped colloidal activated carbon for in situ groundwater treatment. Chem Eng J 191:588–595. https://doi.org/10.1016/j.cej.2012.03.021
6. Mackenzie K, Bleyl S, Kopinke F-D, Doose H, Bruns J (2016) Carbo-iron as improvement of the nanoiron technology: from laboratory design to the field test. Sci Total Environ 563–564:641–648. https://doi.org/10.1016/j.scitotenv.2015.07.107
7. Vogel M, Nijenhuis I, Lloyd J, Boothman C, Pöritz M, Mackenzie K (2018) Combined chemical and microbiological degradation of tetrachloroethene during the application of carbo-iron at a contaminated field site. Sci Total Environ 628–629:1027–1036. https://doi.org/10.1016/j.scitotenv.2018.01.310
8. Mackenzie K, Bleyl S, Georgi A, Kopinke F-D (2012) Carbo-iron—an Fe/AC composite—as alternative to nano-iron for groundwater treatment. Water Res 46:3817–3826. https://doi.org/10.1016/j.watres.2012.04.013
9. Bradley PM, Chapelle FH (2010) Biodegradation of chlorinated ethenes. In: Ward CH, Stroo HF (eds) In situ remediation of chlorinated solvent plumes. Springer, Berlin
10. Bruton TA, Pycke BFG, Halden RU (2015) Effect of nanoscale zero-valent iron treatment on biological reductive dechlorination: a review of current understanding and research needs. Crit Rev Environ Sci Technol 45:1148–1175. https://doi.org/10.1080/10643389.2014.924185
11. Stefaniuk M, Oleszczuk P, Ok YS (2016) Review on nano zerovalent iron (nZVI): from synthesis to environmental applications. Chem Eng J 287:618–632. https://doi.org/10.1016/j.cej.2015.11.046
12. Lee C, Kim JY, Lee WI, Nelson KL, Yoon J, Sedlak DL (2008) Bactericidal effect of zero-valent iron nanoparticles on *Escherichiacoli*. Environ Sci Technol 42:4927–4933. https://doi.org/10.1021/es800408u
13. Diao M, Yao M (2009) Use of zero-valent iron nanoparticles in inactivating microbes. Water Res 43:5243–5251. https://doi.org/10.1016/j.watres.2009.08.051
14. Ševců A, El-Temsah YS, Filip J, Joner EJ, Bobčíková K, Černík M (2017) Zero-valent iron particles for PCB degradation and an evaluation of their effects on bacteria, plants, and soil organisms. Environ Sci Pollut Res 24:21191–21202. https://doi.org/10.1007/s11356-017-9699-5
15. Pawlett M, Ritz K, Dorey RA, Rocks S, Ramsden J, Harris JA (2013) The impact of zero-valent iron nanoparticles upon soil microbial communities is context dependent. Environ Sci Pollut Res 20:1041–1049. https://doi.org/10.1007/s11356-012-1196-2
16. Němeček J, Pokorný P, Lhotský O, Knytl V, Najmanová P, Steinová J, Černík M, Filipová A, Filip J, Cajthaml T (2016) Combined nano-biotechnology for in-situ remediation of mixed contamination of groundwater by hexavalent chromium and chlorinated solvents. Sci Total Environ 563–564:822–834. https://doi.org/10.1016/j.scitotenv.2016.01.019

Czinnerova *et al. Environ Sci Eur*   (2020) 32:154

Page 14 of 15

17. Czinnerová M, Vološčuková O, Marková K, Ševců A, Černík M, Nosek J (2020) Combining nanoscale zero-valent iron with electrokinetic treatment for remediation of chlorinated ethenes and promoting biodegradation: a long-term field study. Water Res 175:115692. https://doi.org/10.1016/j.watres.2020.115692

18. Dolinová I, Štrojsová M, Černík M, Němeček J, Macháčková J, Ševců A (2017) Microbial degradation of chloroethenes: a review. Environ Sci Pollut Res 24:13262–13283. https://doi.org/10.1007/s11356-017-8867-y

19. Löffler FE, Yan J, Ritalahti KM, Adrian L, Edwards EA, Konstantinidis KT, Müller JA, Fullerton H, Zinder SH, Spormann AM (2013) *Dehalococcoides mccartyi* gen. nov., sp. nov., obligately organohalide-respiring anaerobic bacteria relevant to halogen cycling and bioremediation, belong to a novel bacterial class, *Dehalococcoidiaclassis* nov., order Dehalococcoidales ord. nov. and family Dehalococcoidaceae fam. nov., within the phylum Chloroflexi. Int J Syst Evol Microbiol 63:625–635. https://doi.org/10.1099/ijs.0.034926-0

20. Yang Y, Higgins SA, Yan J, Şimşir B, Chourey K, Iyer R, Hettich RL, Baldwin B, Ogles DM, Löffler FE (2017) Grape pomace compost harbors organohalide-respiring *Dehalogenimonas* species with novel reductive dehalogenase genes. ISME J 11:2767

21. Futamata H, Kaiya S, Sugawara M, Hiraishi A (2009) Phylogenetic and transcriptional analyses of a tetrachloroethene-dechlorinating "Dehalococcoides" enrichment culture TUT2264 and its reductive-dehalogenase genes. Microbes Environ 24:330–337. https://doi.org/10.1264/jsme2.ME09133

22. Tiehm A, Schmidt KR (2011) Sequential anaerobic/aerobic biodegradation of chloroethenes—aspects of field application. Curr Opin Biotechnol 22:415–421. https://doi.org/10.1016/j.copbio.2011.02.003

23. Coleman NV, Mattes TE, Gossett JM, Spain JC (2002) Phylogenetic and kinetic diversity of aerobic vinyl chloride-assimilating bacteria from contaminated sites. Appl Environ Microbiol 68:6162–6171. https://doi.org/10.1128/AEM.68.12.6162-6171.2002

24. Mattes TE, Alexander AK, Coleman NV (2010) Aerobic biodegradation of the chloroethenes: pathways, enzymes, ecology, and evolution. FEMS Microbiol Rev 34:445–475. https://doi.org/10.1111/j.1574-6976.2010.00210.x

25. Richards PM, Liang Y, Johnson RL, Mattes TE (2019) Cryogenic soil coring reveals coexistence of aerobic and anaerobic vinyl chloride degrading bacteria in a chlorinated ethene contaminated aquifer. Water Res 157:281–291. https://doi.org/10.1016/j.watres.2019.03.059

26. Mattes TE, Alexander AK, Richardson PM, Munk AC, Han CS, Stothard P, Coleman NV (2008) The genome of *Polaromonas* sp. strain JS666: insights into the evolution of a hydrocarbon- and xenobiotic-degrading bacterium, and features of relevance to biotechnology. Appl Environ Microbiol 74:6405–6416. https://doi.org/10.1128/AEM.00197-08

27. Jennings LK, Chartrand MMG, Lacrampe-Couloume G, Lollar BS, Spain JC, Gossett JM (2009) Proteomic and transcriptomic analyses reveal genes upregulated by cis-dichloroethene in *Polaromonas* sp. strain JS666. Appl Environ Microbiol 75:3733–3744. https://doi.org/10.1128/AEM.00031-09

28. Bewley R, Hick P, Rawcliffe A (2015) Meeting the challenges for bioremediation of chlorinated solvents at operational sites: a comparison of case studies. In: Proceeding of the 13th international UFZ-Deltarez conference on sustainable use and management of soil sediment and water resources. Copenhagen, Denmark

29. Dolinová I, Czinnerová M, Dvořák L, Stejskal V, Ševců A, Černík M (2016) Dynamics of organohalide-respiring bacteria and their genes following in-situ chemical oxidation of chlorinated ethenes and biostimulation. Chemosphere 157:276–285. https://doi.org/10.1016/j.chemosphere.2016.05.030

30. Nechanická M, Dvořák L, Dolinová I (2018) Use of nanofiber carriers for monitoring of microbial biomass. In: Topical issues of rational use of natural resources: proceedings of the international Forum-Contest of Young Researchers, April 18–20, 2018, St. Petersburg, Russia. CRC Press, p 361

31. Caporaso JG, Lauber CL, Walters WA, Berg-Lyons D, Lozupone CA, Turnbaugh PJ, Fierer N, Knight R (2011) Global patterns of 16S rRNA diversity at a depth of millions of sequences per sample. Proc Natl Acad Sci 108:4516–4522. https://doi.org/10.1073/pnas.1000080107

32. Caporaso JG, Lauber CL, Walters WA, Berg-Lyons D, Huntley J, Fierer N, Owens SM, Betley J, Fraser L, Bauer M, Gormley N, Gilbert JA, Smith G, Knight R (2012) Ultra-high-throughput microbial community analysis on the Illumina HiSeq and MiSeq platforms. ISME J 6:1621–1624. https://doi.org/10.1038/ismej.2012.8

33. Kozich JJ, Westcott SL, Baxter NT, Highlander SK, Schloss PD (2013) Development of a dual-index sequencing strategy and curation pipeline for analyzing amplicon sequence data on the MiSeq Illumina sequencing platform. Appl Environ Microbiol 79:5112–5120. https://doi.org/10.1128/AEM.01043-13

34. Callahan BJ, McMurdie PJ, Rosen MJ, Han AW, Johnson AJA, Holmes SP (2016) DADA2: high-resolution sample inference from Illumina amplicon data. Nat Methods 13:581–583. https://doi.org/10.1038/nmeth.3869

35. Oksanen J, Blanchet FG, Friendly M, Kindt R, Legendre P, McGlinn D, Minchin PR, O'Hara RB, Simpson GL, Solymos P, Stevens MHH, Szoecs E, Wagner H (2014) Vegan: community ecology package version 2.5–6 from CRAN. https://rdrr.io/cran/vegan/. Accessed 25 Mar 2020

36. McMurdie PJ, Holmes S (2013) phyloseq: an R package for reproducible interactive analysis and graphics of microbiome census data. PLoS ONE 8:e61217. https://doi.org/10.1371/journal.pone.0061217

37. Němeček J, Pokorný P, Lacinová L, Černík M, Masopustová Z, Lhotský O, Filipová A, Cajthaml T (2015) Combined abiotic and biotic in-situ reduction of hexavalent chromium in groundwater using nZVI and whey: a remedial pilot test. J Hazard Mater 300:670–679. https://doi.org/10.1016/j.jhazmat.2015.07.056

38. Stumm W, Morgan JJ (1996) Aquatic chemistry: chemical equilibria and rates in natural waters, 3rd edn. Wiley and Sons, New York

39. Bouwer EJ (2017) Bioremediation of chlorinated solvents using alternate electron acceptors. In: Handb Bioremediation 1993. https://www.taylorfrancis.com/. Accessed 9 Mar 2020

40. Xu Y, Xue L, Ye Q, Franks AE, Zhu M, Feng X, Xu J, He Y (2018) Inhibitory effects of sulfate and nitrate reduction on reductive dechlorination of PCP in a flooded paddy soil. Front Microbiol 9:567. https://doi.org/10.3389/fmicb.2018.00567

41. Němeček J, Steinová J, Špánek R, Pluhař T, Pokorný P, Najmanová P, Knytl V, Černík M (2018) Thermally enhanced in situ bioremediation of groundwater contaminated with chlorinated solvents—a field test. Sci Total Environ 622–623:743–755. https://doi.org/10.1016/j.scitotenv.2017.12.047

42. Matturro B, Ubaldi C, Rossetti S (2016) Microbiome dynamics of a polychlorobiphenyl (PCB) historically contaminated marine sediment under conditions promoting reductive dechlorination. Front Microbiol 7:1502. https://doi.org/10.3389/fmicb.2016.01502

43. Yamazawa A, Date Y, Ito K, Kikuchi J (2014) Visualizing microbial dechlorination processes in underground ecosystem by statistical correlation and network analysis approach. J Biosci Bioeng 117:305–309. https://doi.org/10.1016/j.jbiosc.2013.08.010

44. Sheu YT, Chen SC, Chien CC, Chen CC, Kao CM (2015) Application of a long-lasting colloidal substrate with pH and hydrogen sulfide control capabilities to remediate TCE-contaminated groundwater. J Hazard Mater 284:222–232. https://doi.org/10.1016/j.jhazmat.2014.11.023

45. Brzeszcz J, Kapusta P, Steliga T, Turkiewicz A (2020) Hydrocarbon removal by two differently developed microbial inoculants and comparing their actions with biostimulation treatment. Molecules 25:661. https://doi.org/10.3390/molecules25030661

46. Kotik M, Davidová A, Voříšková J, Baldrian P (2013) Bacterial communities in tetrachloroethene-polluted groundwaters: a case study. Sci Total Environ 454–455:517–527. https://doi.org/10.1016/j.scitotenv.2013.02.082

47. Guan X, Liu F, Xie Y, Zhu L, Han B (2013) Microbiota associated with the migration and transformation of chlorinated aliphatic hydrocarbons in groundwater. Environ Geochem Health 35:535–549. https://doi.org/10.1007/s10653-013-9513-3

48. Paes F, Liu X, Mattes TE, Cupples AM (2015) Elucidating carbon uptake from vinyl chloride using stable isotope probing and Illumina sequencing. Appl Microbiol Biotechnol 99:7735–7743. https://doi.org/10.1007/s00253-015-6606-1

49. Tsai TT, Liu JK, Chang YM, Chen KF, Kao CM (2014) Application of polycolloid-releasing substrate to remediate trichloroethylene-contaminated groundwater: a pilot-scale study. J Hazard Mater 268:92–101. https://doi.org/10.1016/j.jhazmat.2014.01.004

50. Atashgahi S, Lu Y, Smidt H (2016) Overview of known organohalide-respiring bacteria—phylogenetic diversity and environmental distribution. In: Adrian L, Löffler FE (eds) Organohalide-respiring bacteria. Springer, Berlin, pp 63–105

Czinnerova *et al. Environ Sci Eur*   (2020) 32:154

Page 15 of 15

51. Němeček J, Dolinová I, Macháčková J, Špánek R, Ševců A, Lederer T, Černík M (2017) Stratification of chlorinated ethenes natural attenuation in an alluvial aquifer assessed by hydrochemical and biomolecular tools. Chemosphere 184:1157–1167. https://doi.org/10.1016/j.chemosphere.2017.06.100

52. Liang Y, Liu X, Singletary MA, Wang K, Mattes TE (2017) Relationships between the abundance and expression of functional genes from vinyl chloride (VC)-degrading bacteria and geochemical parameters at VC-contaminated sites. Environ Sci Technol 51:12164–12174. https://doi.org/10.1021/acs.est.7b03521

53. Němeček J, Marková K, Špánek R, Antoš V, Kozubek P, Lhotský O, Černík M (2020) Hydrochemical conditions for aerobic/anaerobic biodegradation of chlorinated ethenes—a multi-site assessment. Water 12:322. https://doi.org/10.3390/w12020322

Publisher's Note

Springer Nature remains neutral with regard to jurisdictional claims in published maps and institutional affiliations.